



Ag nanoparticles on mixed Al₂O₃–Ga₂O₃ supports as catalysts for the N-alkylation of amines with alcohols

Inge Geukens^a, Frederik Vermoortele^a, Maria Meledina^b, Stuart Turner^b, Gustaaf Van Tendeloo^b, Dirk E. De Vos^{a,*}

^a Department of Microbial and Molecular Systems, KU Leuven, Centre for Surface Chemistry and Catalysis, Kasteelpark Arenberg 23, 3001 Leuven, Belgium

^b Electron Microscopy for Materials Science (EMAT), University of Antwerp, Groenenborgerlaan 171, 2020 Antwerp, Belgium



ARTICLE INFO

Article history:

Received 6 August 2013

Received in revised form

25 September 2013

Accepted 28 September 2013

Available online 9 October 2013

Keywords:

Alcohol amination

Silver

Nanoparticles

Heterogeneous catalysis

Support influence

ABSTRACT

The combination of AgNO₃ with NaH results in Ag nanoparticles that can selectively perform alcohol aminations under mild reaction conditions (110 °C). NaH not only serves as a reducing agent for the Ag salt, but also activates the alcohol for dehydrogenation to the corresponding ketone/aldehyde. The stability of the particles can be improved by immobilizing them onto mixed Al₂O₃–Ga₂O₃ supports; the combination of Ga and Al provides materials with stronger Lewis acidic sites compared to pure alumina or gallium oxide supports. This leads to catalysts with enhanced activities, without the necessity of adding external Lewis acids. Detailed TEM characterization also reveals a close interaction between the Ag NPs and the gallium oxide phase. The obtained catalysts are recyclable and show activity for the alcohol amination using a variety of aliphatic and aromatic amines under mild conditions.

© 2013 Elsevier B.V. All rights reserved.

1. Introduction

Functionalized secondary or tertiary amines are important intermediates for pharmaceuticals, polymers, dyes and electronic materials [1–5]. Catalytic C–N coupling of amines with alkyl or aryl halides allows selective synthesis of these higher amines (Fig. 1a) [2,6,7]. We recently showed that Ni nanoparticles in phosphonium ionic liquids are excellent catalysts for these reactions, even using aryl chlorides [8]. Nevertheless, halide salts are formed as side products (Fig. 1a). Working with widely available alcohols solves this problem, as H₂O is the only side product (Fig. 1b) [9]. A downside of using alcohols is that hydroxyl groups are poor leaving groups, especially compared with halides. Therefore, the commonly applied reaction sequence is the “hydrogen borrowing” cycle (Fig. 2). First, the alcohol is dehydrogenated over the metal catalyst to form a carbonyl compound, which reacts with the amine to form an imine and water. The imine is reduced to the alkylated amine product, thereby reoxidizing the catalyst. The metal thus “borrows” the hydrogen atoms from the alcohol to reduce the imine [9]. A downside to this cycle is that tertiary alcohols are not able to react. Catalysts for the hydrogen borrowing reaction include homogeneous Ru or Ir complexes [9,10]. There is a trend to use

less expensive elements such as Cu [11], Fe [12], Ni [13], or combinations thereof [14,15]. Raney Ni has often been used, though quite drastic reaction conditions are necessary, such as an over-stoichiometric amount of the catalyst (200 mol%) or of the alcohol (500 mol%), or high temperatures [10].

One element which has gained attention lately is Ag. This relatively inexpensive metal shows remarkable activity and selectivity for the coupling of alcohols and amines. The lower stability of the Ag–H bond compared to that of other noble elements (Au, Pd, Pt) is thought to facilitate the imine reduction [16]. In using Ag nanoparticles on Al₂O₃, Shimizu found a synergistic effect between the acid–base sites of Al₂O₃ and the Ag sites [16,17]; even then, high temperatures (140 °C) were required and the addition of Lewis acids like FeCl₃·6H₂O was necessary to facilitate the imine reduction. Moreover, the catalysts were only applied to anilines [16]. Later catalysts, e.g. Cu_{0.95}Ag_{0.05} on Al₂O₃, were applicable to a broader substrate range and did not require Lewis acids, but even higher temperatures were used (155 °C) [18]. Deng's Ag₆Mo₁₀O₃₃ catalyst for the alkylation of amines, carboxamides and sulfonamides with alcohols requires high temperatures (160 °C) and the addition of 20 mol% of KOtBu [19]. Finally, by increasing the surface area of the Al₂O₃ and decreasing the Ag particle size, the reaction can be conducted with smaller amounts of Ag/Al₂O₃ catalyst and in milder reaction conditions (120 °C), but a base like Cs₂CO₃ (20 mol%) is still essential for high yields [20]. These examples show that despite the favourable interactions between the Ag metal and

* Corresponding author. Tel.: +32 16 321639.

E-mail address: dirk.devos@biw.kuleuven.be (D.E. De Vos).

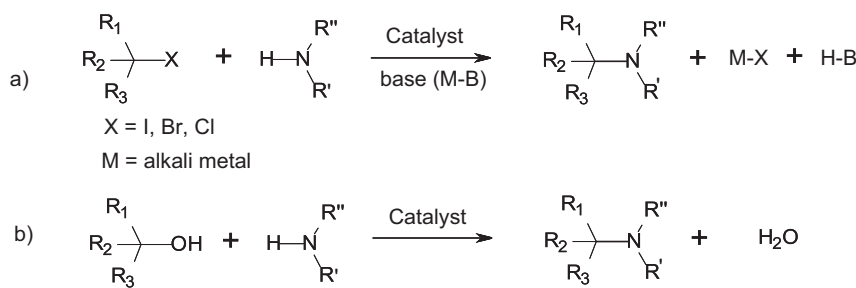


Fig. 1. *N*-alkylation reactions of amines with (a) alkyl or aryl halides and (b) alcohols.

supports like Al_2O_3 , efficient catalysis still often requires extra additives, like bases or Lewis acids.

In this paper, we first examine the use of unsupported Ag nanoparticles in the reaction of 4-ethylaniline and benzyl alcohol. While significant yield improvements can be realized by changing the nanoparticle preparation and reaction procedures, the stability of the nanoparticles under reaction conditions calls for use of a support. By changing the acid–base properties of the support, we succeed not only in increasing the reaction rate in mild reaction conditions (110°C); moreover, the use of additives becomes superfluous. Finally, the substrate scope of the new $\text{Ag}/\text{Al}_2\text{O}_3\text{-Ga}_2\text{O}_3$ catalysts was explored by testing a variety of aromatic and aliphatic amines and alcohols.

2. Experimental

2.1. General

Reactions were carried out under inert atmosphere in dried, magnetically stirred glass reaction vials (8 mL) with reflux setup. Reaction mixtures were analyzed with a Shimadzu 2014 GC equipped with a CP Sil-8 column and a FID detector using *n*-tetradecane as internal standard. Mass spectra were obtained on an Agilent 6890N GC with a HP-5MS column coupled to a 5973 MSD mass spectrometer. Samples for TEM investigation were prepared by crushing the powders with ethanol in a mortar and placing several drops of the suspension onto a holey carbon grid. TEM and HRTEM investigations were performed on a JEOL 3000F transmission electron microscope, operated at 300 kV. HAADF-STEM and EDX analysis were performed using a FEI Titan “cubed” microscope, equipped with an aberration corrector for the probe-forming lens and a Super-X, large solid-angle EDX detector, operated at 120 kV. Powder X-ray diffraction (PXRD) patterns were measured with a STOE COMBI P diffractometer in high throughput mode using a Cu $\text{K}\alpha_1$ source (1.5406 Å) with 2θ ranging from -15 to 62° . ICP-AES

analysis of the materials was performed on an Ultima apparatus equipped with a Burgener atomizer and a radial optic detector, using Ar as carrier gas and as plasma. N_2 physisorption experiments were performed after pretreatment in N_2 at 423 K on a Micromeritics Tristar apparatus at 77 K . FT-IR measurements were performed with a Nicolet 6700 spectrometer, using a self-supporting sample wafer. The sample was pretreated at 798 K in air. After cooling to room temperature, 20 mbar pyridine was introduced and allowed to adsorb on the sample. The FT-IR spectrum was measured after temperature programmed desorption (5 K/min) at 423 K . Amines, alcohols and solvents were used as received from Sigma–Aldrich.

2.2. Reaction procedure with unsupported Ag NPs

Representative example (Table 2, entry 3): 0.054 mmol AgNO_3 (9.2 mg), 0.5 mmol NaH (60% dispersion in mineral oil; 12 mg) and 0.5 mL of toluene were mixed in a vial; the Ag NPs were formed by heating this mixture to 110°C under reflux for 1 h. 1.8 mmol of 4-ethylaniline (220 μl) and 1.8 mmol benzyl alcohol (190 μl) were added and the reaction mixture was heated to 110°C for 20 h. After cooling and centrifugation, the supernatant was isolated, washed with water to remove inorganic impurities and analyzed by GC and GC-MS.

2.3. Synthesis of the materials

2.3.1. Ag supported on commercial $\gamma\text{-Al}_2\text{O}_3$ via wet impregnation

Following a literature recipe [16], 37.1 mg AgNO_3 was dissolved in 15 ml of water and this solution was used to suspend 977 mg of a commercial $\gamma\text{-Al}_2\text{O}_3$ support (crushed Saint-Gobain NorPro® Unispheres®; BET $227\text{ m}^2/\text{g}$). After stirring for 4 h at room temperature, the water was evaporated at $80\text{--}100^\circ\text{C}$. The sample was calcined at 600°C for 1 h ($10^\circ\text{C}/\text{min}$). This material is referred to as $\text{Ag}(2.4\text{ wt\%})/\gamma\text{-Al}_2\text{O}_3$ commercial. Part of the Ag-loaded, calcined $\gamma\text{-Al}_2\text{O}_3$ was reduced in a H_2 flow for 30 min at 300°C and the other part was reduced with NaH .

2.3.2. Ag supported on $\gamma\text{-Al}_2\text{O}_3$ via *in situ* sol-gel synthesis

Following a literature recipe [20], 4.17 ml aluminium tri-sec-butoxide was added to 31.5 mg AgNO_3 together with 0.99 ml 2-butanol, followed by stirring until the AgNO_3 was completely dissolved and a gel was formed. The gel was stirred for 3 h at 100°C , after which 2.25 ml H_2O was added dropwise, followed by stirring for 1 h at 100°C . The resulting brown–black solid was centrifuged, washed with acetone (3×), dried at 100°C overnight and finally calcined at 600°C for 1 h ($10^\circ\text{C}/\text{min}$). This material is referred to as $\text{Ag}(2.4\text{ wt\%})/\gamma\text{-Al}_2\text{O}_3$ sol-gel. The material was reduced with NaH , or with H_2 (30 min, 300°C).

2.3.3. Preparation of the $\text{Ag}/\text{Al}_2\text{O}_3\text{-Ga}_2\text{O}_3$ series

Representative example $\text{Ag}/\text{Al}_2\text{O}_3\text{-Ga}_2\text{O}_3$ (0.6) (Table 4, entry 4): following a literature procedure [21], 1.394 g of $\text{Ga}(\text{NO}_3)_3\text{:xH}_2\text{O}$ and

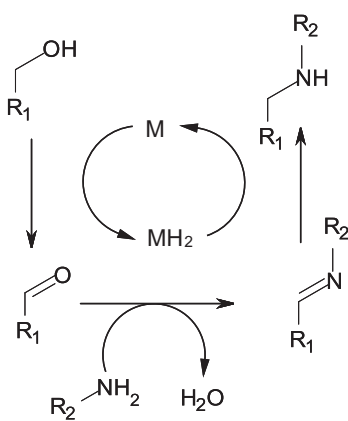


Fig. 2. The hydrogen borrowing cycle.

1.125 g of $\text{Al}(\text{NO}_3)_3 \cdot 9\text{H}_2\text{O}$ were dissolved in 15 ml of water. This solution was added very quickly to a vigorously stirred $(\text{NH}_4)_2\text{CO}_3$ aqueous solution (5.1 g $(\text{NH}_4)_2\text{CO}_3$ in 30 ml H_2O) and stirred for 1 h. The precipitate was centrifuged, washed with water ($2\times$) and ethanol ($2\times$), and dried at 80 °C after which the sample was calcined at 700 °C for 3 h (5 °C/min). The material was then loaded with Ag via the wet impregnation technique: 5 ml of a 0.028 M AgNO_3 aqueous solution was added to 300 mg of the as-synthesized support, stirred for 4 h at room temperature, followed by water evaporation at 80–100 °C and calcination at 600 °C for 1 h (10 °C/min). The other mixed or pure oxides were prepared in similar ways, by adjusting the quantities of the nitrate salts (see supporting information for more details). The materials are denoted as $\text{Ag}/\text{Al}_2\text{O}_3-\text{Ga}_2\text{O}_3$ (x), with x the $\text{Ga}/(\text{Ga}+\text{Al})$ content.

2.4. Reaction procedure with the supported Ag NPs

Representative example (Table 5, entry 1): Prior to use, the catalyst (162 mg; 3 mol%) was dried at 150 °C. Then, NaH (60% dispersion in mineral oil; 12 mg) and 1 ml of toluene were added, followed by 1 h heating at 110 °C. 1.8 mmol of 4-ethylaniline (220 μl) and 3.6 mmol benzyl alcohol (380 μl) were added. After 26 h reaction at 110 °C, analysis was performed as in Section 2.2. To recycle the catalyst, the material was washed with water after reaction to remove inorganic impurities, followed by washing with 2-propanol ($2\times$) and acetone ($2\times$). The material was dried overnight at 150 °C after which again NaH (0.5 mmol; 12 mg) was added and a new run was started.

3. Results and discussion

3.1. Reactions with metal nanoparticles

In the search for an economically favourable catalyst that is able to selectively perform a wide variety of alcohol aminations under mild conditions, nickel nanoparticles (NPs) were used as starting point. These were synthesized by the reduction of a nickel salt in toluene with NaH in the presence of lithium *tert*-butoxide (LiOtBu). Such nanoparticles were previously used successfully for the racemization of primary amines [22], a reaction with mechanistic similarities to the hydrogen borrowing cycle. The nickel particles were applied for the coupling of benzyl alcohol (**1**) and 4-ethylaniline (**2**) (Fig. 3). A frequent reoccurring side product is the imine (**4**), which is formed when the final step of the hydrogen borrowing cycle does not take place. If this is the case, the hydrogen atoms adsorbed on the Ag surface need to be removed in order to close the mass and redox balance, e.g. as hydrogen gas (Fig. 2).

Preliminary results using NiBr_2 as metal precursor showed indeed some conversion (31%), but with only 10% selectivity for the secondary amine **3**, the remainder being the imine (**4**; Table 1, entry 1). Using another nickel precursor even lowered the conversion (Table 1, entry 2). Because of the poor selectivity with nickel, we tested other elements, employing the same synthesis procedure for the particle formation. As can be seen from Table 1, the selectivity did not improve when using Fe or Cu nanoparticles, the imine being the dominant product. Ag, on the other hand, showed markedly better selectivities of up to 93% for the alkylated amine **3** (Table 1, entries 7–8). Of the different tested precursors, AgNO_3 seemed to provide the best results and was used for further optimization.

In a next step, the influence of the different additives of the Ag nanoparticle system, i.e. LiOtBu and NaH, on the reaction was examined (Table 2). This showed that the presence of LiOtBu is not necessary for the activity of the NPs (Table 2, entry 2–3). Other bases were also tested (see supporting information), but none gave

Table 1

Application of Ni, Fe, Cu and Ag NPs in the *N*-alkylation of 4-ethylaniline with benzyl alcohol.^a

Entry	Metal precursor	$X_2 (\%)^b$	$S_3 (\%)^c$	$S_4 (\%)^d$
1	NiBr_2	31	10	90
2	$\text{Ni}(\text{acac})_2$	6	8	90 ^e
3	FeCl_3	6	4	93 ^e
4	$\text{Fe}(\text{OAc})_2$	6	7	90 ^e
5	CuCl_2	12	12	87 ^e
6	$\text{Cu}(\text{OAc})_2$	14	12	86 ^e
7	AgOAc	34	93	7
8	AgNO_3	37	93	7

^a Reaction conditions: benzyl alcohol (**1**, 1.8 mmol), 4-ethylaniline (**2**, 1.8 mmol), metal precursor (0.054 mmol, 3 mol%), lithium *tert*-butoxide (LiOtBu ; 0.054 mmol), NaH (0.5 mmol), toluene (0.5 ml), 110 °C, 20 h, Ar.

^b Conversion of **2**.

^c Selectivity for **3**.

^d Selectivity for **4**.

^e Other identified products (GC-MS): benzyl benzoate and 4,4'-diethylazobenzene.

better results than in the absence of an extra base. It was also shown that AgNO_3 or NaH alone cannot catalyze the reaction; their combination is essential for catalytic activity (Table 2, entries 4–5). Besides reducing the Ag^+ , excess NaH also easily deprotonates the benzyl alcohol, which is the compound with the lowest pK_a in the mixture. This results in the formation of an alkoxide, as was also visually observed by H_2 gas formation when adding the alcohol. To further examine this, the reaction was also performed by first mixing amine, alcohol and NaH prior to addition of AgNO_3 (entry 6). In such case, no hydride is left, since the benzyl alcohol is present in excess with respect to NaH. Nevertheless, an immediate reduction of the Ag^+ was observed, with formation of a black suspension. This suggests that in this case, the alkoxide is supplying the electrons for the Ag reduction while it is simultaneously dehydrogenated to a carbonyl compound. With this procedure, the same conversion was obtained after 20 h, though selectivity was significantly lower, indicating that the pre-reduction of the Ag salt with NaH is still preferred (entry 6). The amount of NaH used is also important: adding less NaH did not significantly affect conversion, but lowered selectivity (entry 7). With a large excess of NaH, both

Table 2

Influence of the precursors and additives on the amine alkylation catalyzed by Ag NPs.^a

	AgNO_3	NaH (mmol)	1:2 ^b	$X_2 (\%)^c$	$S_3 (\%)^d$	$S_4 (\%)^e$
1	–	–	1:1	0.2	0	32
2 ^f	AgNO_3	NaH (0.5)	1:1	37	93	7
3	AgNO_3	NaH (0.5)	1:1	38	95	5
4	AgNO_3	–	1:1	1	8	3
5	–	NaH (0.5)	1:1	1	8	83
6 ^g	AgNO_3	NaH (0.5)	1:1	37	51	48
7	AgNO_3	NaH (0.25)	1:1	34	86	14
8	AgNO_3	NaH (0.75)	1:1	19	64	36
9	AgNO_3	NaH (0.5)	1:2	48 ^h	95	5
10	AgNO_3	NaH (0.5)	2:1	56	95	5
11	AgNO_3	NaH (0.5)	3:1	58	91	9
12	AgNO_3	NaH (0.5)	4:1	64	74	26
13 ⁱ	AgNO_3	NaH (0.5)	1:1	9	36	64

^a Reaction conditions as in Table 1, but without LiOtBu .

^b Molar ratio of benzyl alcohol (**1**) to 4-ethylaniline (**2**).

^c Conversion of **2**.

^d Selectivity for **3**.

^e Selectivity for **4**.

^f 0.054 mmol of LiOtBu was added.

^g 0.5 ml toluene, **1** (1.8 mmol), **2** (1.8 mmol) and 0.5 mmol NaH were mixed and then added to 0.054 mmol AgNO_3 ; 20 h, 110 °C, Ar.

^h Conversion of **1**.

ⁱ After recycling of the catalyst, second run.

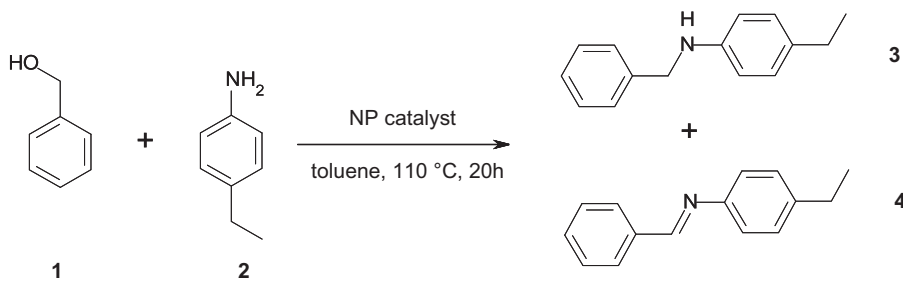


Fig. 3. *N*-alkylation of 4-ethylaniline (**2**) with benzyl alcohol (**1**) to form *N*-benzyl-4-ethylaniline (**3**), with the imine (**4**) as the side product.

Table 3

Effect of the reduction procedure for Ag/ γ -Al₂O₃ catalysts.^a

Catalyst	Reducing agent	X ₂ (%) ^b	S ₃ (%) ^c	S ₄ (%) ^d
1 ^e Ag(2.4 wt%)/ γ -Al ₂ O ₃ commercial	NaH	44	94	6
2 ^e Ag(2.4 wt%)/ γ -Al ₂ O ₃ commercial	H ₂	5	27	73
3 ^f Ag(2.4 wt%)/ γ -Al ₂ O ₃ sol-gel	NaH	41	88	11
4 ^f Ag(2.4 wt%)/ γ -Al ₂ O ₃ sol-gel	H ₂	15	53	47

^a Reaction conditions: 2.4 mol% Ag catalyst, reduced with 0.5 mmol NaH or using a hydrogen stream (30' at 300 °C); 1 mL toluene, **1** (3.6 mmol), **2** (1.8 mmol), 20 h, 110 °C, Ar.

^b Conversion of **2**.

^c Selectivity for **3**.

^d Selectivity for **4**.

^e Synthesis by wet impregnation of a commercial γ -Al₂O₃ support.

^f The Ag NPs are entrapped in an in situ sol-gel synthesis of the alumina support (see Section 2).

conversion and selectivity were significantly lowered (entry 8). The optimum amount of NaH for which the highest yield was obtained was 0.5 mmol for a reaction at the 1.8 mmol scale (entry 3). The double role of NaH, as reducing agent and as base, is in line with other Ag systems, which need extra base to facilitate the alcohol dehydrogenation [20].

Despite the good selectivity of the Ag NPs, the conversion was still too low (Table 2, entry 3). Therefore, the alcohol: amine ratio was adjusted. An alcohol: amine ratio of 2:1 provided the best conversion and selectivity (entry 10). With a larger excess of alcohol, selectivity was negatively affected (Table 2, entries 11–12). Prolonging the reaction for more than 20 h did not increase the yield any further, showing that the particles lose most of their activity during reaction. This is due to aggregation and precipitation of the particles, as was observed visually, and was also shown by the drastic drop in activity after recycling of the Ag catalyst (Table 2, entry 13). Attempts to stabilize the particles by polymer addition were not successful (see supporting information). For this reason, the focus was placed on using oxide supports to enhance the stability of the particles and, simultaneously, boost their activity.

Table 4

Characteristics of the Ag/Al₂O₃–Ga₂O₃ materials and their turnover frequency (TOF) for the *N*-alkylation reaction.^a

Catalyst	Ag content (wt%)	Ga/(Ga + Al)	BET surface area (m ² /g) with Ag	BET surface area (m ² /g) without Ag	TOF (1/h) ^b
1 Ag/Al ₂ O ₃ (0)	3.1	0	94	152	0.64
2 ^c Ag/ γ -Al ₂ O ₃ commercial	5.4	0	n.d.	227	0.68
3 Ag/Al ₂ O ₃ –Ga ₂ O ₃ (0.3)	4.4	0.3	149	197	1.07
4 Ag/Al ₂ O ₃ –Ga ₂ O ₃ (0.6)	4.0	0.6	108	138	1.32
5 Ag/Al ₂ O ₃ –Ga ₂ O ₃ (0.8)	3.6	0.8	68	110	1.63
6 Ag/Ga ₂ O ₃ (1)	3.2	1	15	24	1.44
7 ^d Ag NPs	–	–	–	–	0.74

^a Reaction conditions: 1.7 mol % Ag catalyst (0.03 mmol Ag), 0.5 mmol NaH, 1 mL toluene, **1** (3.6 mmol), **2** (1.8 mmol), 20 h, 110 °C, Ar.

^b Mole of product (**3**) formed per mole of Ag per h after 20 h.

^c Commercial γ -Al₂O₃ support loaded with Ag by wet impregnation.

^d 0.03 mmol AgNO₃ (5.2 mg) was used. n.d.: not determined.

3.2. Reactions with Ag on mixed oxides

As a starting point, the Ag/ γ -Al₂O₃ catalysts used in literature were reproduced and activated by reduction under flowing H₂ [16,17]. To compare the reduction methods, the materials were also reduced with NaH. As shown in Table 3, NaH clearly gives better catalytic results, irrespective of the method used to prepare the catalyst. For the heterogenized catalyst, an additional role of NaH could be to deprotonate the surface hydroxyl groups of γ -Al₂O₃. This would increase the local basicity and enhance the catalyst's activity.

To further enhance the activity, gallium was introduced into the oxide support. Similar Al₂O₃–Ga₂O₃ mixed oxides have been investigated for reactions such as the reduction of NO_x by methane [23,24]. Comparing the acid-base properties of a mixed Al₂O₃–Ga₂O₃ oxide with those of pure Al₂O₃, it has been found that a larger number of strong Lewis acidic sites is created by the presence of Ga [23]. The Al₂O₃–Ga₂O₃ materials have a local superficial spinel structure which differs significantly from bulk Ga₂O₃, also leading to enhanced Lewis acidity compared to pure Ga₂O₃ [24]. The mixed supports were prepared by coprecipitation, with fast addition of Al(NO₃)₃ and Ga(NO₃)₃ to an aqueous (NH₄)₂CO₃ solution, followed by calcination of the precipitate [25]. The Ga/(Ga + Al) ratios were varied in the Al₂O₃–Ga₂O₃ series between 0 (pure Al₂O₃) and 1 (pure Ga₂O₃). XRD confirmed that the crystal structures of the Al₂O₃–Ga₂O₃ mixed oxides were similar to those reported in literature (supporting information) [25]. Strikingly, the aluminas and the solid solutions have much higher specific surface areas than pure Ga₂O₃ (Table 4). Finally, Fourier transform infrared (FT-IR) spectroscopy with pyridine chemisorption, e.g. on Al₂O₃–Ga₂O₃ (0.8), confirmed the presence of Lewis acid sites (supporting information).

Next, the materials were loaded with Ag via wet impregnation, followed by calcination at 600 °C. Some compositional and physicochemical characteristics of the obtained Ag catalysts are summarized in Table 4 (entries 1–6; see also supporting information). For all materials, the surface areas decreased after

Table 5N-alkylations of amines with alcohols catalyzed by Ag/Al₂O₃–Ga₂O₃ (0.8).^a

Entry	Alcohol	Amine	X_6 (%) ^b	S_7 (%) ^c	S_8 (%) ^d	S_9 (%) ^e
5	6	7	8	9	.	.
1 ^g			84	96	3	–
2 ^h			58	93	6	–
3 ^g			85	96	3	–
4 ^f			75	36	58	6
5 ^{f,g}			56	14	–	79
6 ^g		$\text{CH}_3(\text{CH}_2)_5\text{NH}_2$	86	17	83	–
7 ^f		$\text{CH}_3(\text{CH}_2)_7\text{NH}_2$	72	14	83	3
8	$\text{CH}_3(\text{CH}_2)_7\text{OH}$		20	54	42	4
9	$\text{CH}_3(\text{CH}_2)_5\text{OH}$		15	53	44	3
10 ^f	$\text{CH}_3(\text{CH}_2)_7\text{OH}$	$\text{CH}_3(\text{CH}_2)_7\text{NH}_2$	25	–	96	4

^a Reaction conditions: 3 mol% Ag catalyst, 0.5 mmol NaH, 1 mL toluene, alcohol (3.6 mmol), amine (1.8 mmol), 26 h, 110 °C, Ar.^b Conversion of **6**.^c Selectivity for **7**.^d Selectivity for **8**.^e Selectivity for **9**.^f 48 h.^g Other identified products (GC-MS): benzyl benzoate.^h Other identified products (GC-MS): benzoic acid, 4-methyl-, (4-methylphenyl)methyl ester.

Ag loading. High resolution transmission electron microscopy (HRTEM) and high-angle annular dark-field scanning transmission electron microscopy (HAADF STEM), e.g. performed on the Ag/Al₂O₃–Ga₂O₃ (0.8) sample, showed that the Ga and Al are indeed present as oxides in the material, whereas the spherical Ag particles are present in their metallic form (Fig. 4). This was further confirmed by energy-dispersive X-ray spectroscopy (EDX) mapping, in Fig. 5, showing the dispersion of the Ag nanoparticles in the Al₂O₃–Ga₂O₃ matrix. In some cases, the Ag nanoparticles are covered by a partially crystalline shell (see for example the layered structure indicated by arrows in Fig. 4b), which was shown to be Ga_xO_y by spatially resolved electron energy-loss spectroscopy (see supplementary information).

Finally, the supported Ag catalysts were tested for their activity in the reference N-alkylation (Fig. 3), using the optimum 2:1

alcohol:amine ratio. Averaged turnover frequencies after 20 h are displayed in Table 4, together with data for the reaction with the unsupported Ag NPs in the same conditions. Immobilizing the Ag particles clearly improves their activity, as all supported Ag catalysts displayed higher TOFs than unsupported Ag NPs, except when the support was Al₂O₃, either self-prepared or from a commercial source (entries 1 and 2). This can be attributed to a suitable stabilization of the Ag NPs on the high surface area mixed oxides, but also to a synergistic action between the Ag sites and the Lewis acid sites of the Ga-containing supports [16,17]. The Lewis acidity of the support could improve the activity of the Ag NPs in various ways. First, Lewis acidity could result in the withdrawal of some electron density from the metal NPs towards the metal–support interface, which would facilitate the alcohol dehydrogenation on the Ag [26]. The close proximity of Lewis acid sites and Ag sites could also provide

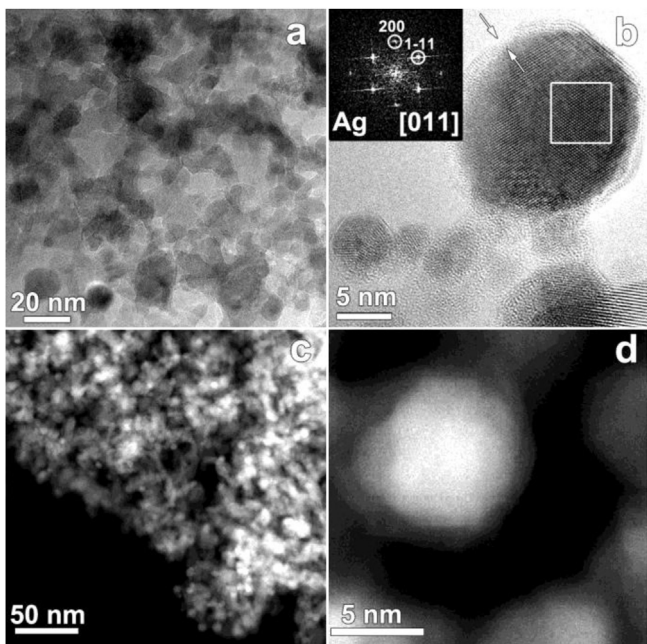


Fig. 4. (a) TEM image of the $\text{Ag}/\text{Al}_2\text{O}_3-\text{Ga}_2\text{O}_3$ (0.8) sample. The sample consists of strongly agglomerated, non-uniform nanoparticles. Spherical Ag nanoparticles (dark contrast features) are spread throughout the agglomerates; (b) HRTEM image of a Ag nanoparticle imaged along the $[0\ 1\ 1]$ zone axis, as evidenced by the inset FT. The white square indicates the area of the FT; (c) HAADF STEM image of the $\text{Ag}/\text{Al}_2\text{O}_3-\text{Ga}_2\text{O}_3$ (0.8) sample. Ag nanoparticles are seen as bright contrast features and (d) HAADF STEM image of a single Ag nanoparticle. The nanoparticles have a near-spherical shape and are generally covered by a 1–2 nm partially crystalline Ga_xO_y shell.

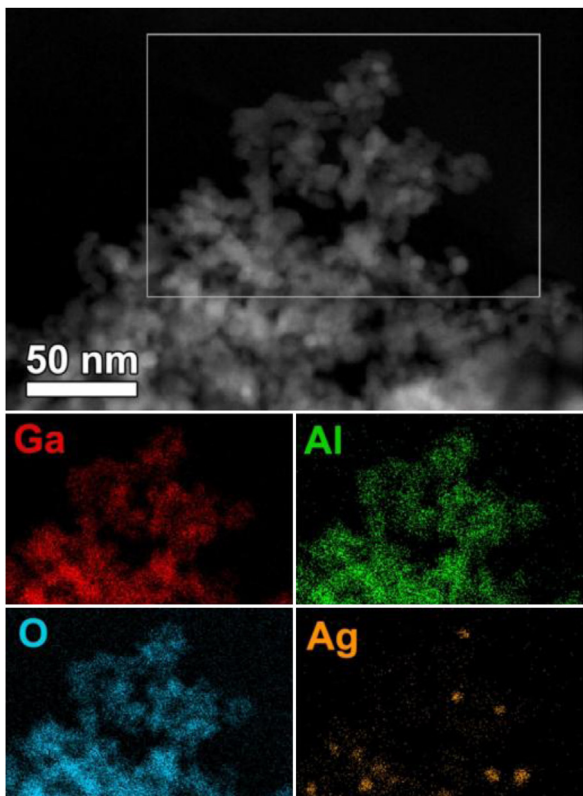


Fig. 5. HAADF STEM image and EDX maps of the $\text{Ag}/\text{Al}_2\text{O}_3-\text{Ga}_2\text{O}_3$ (0.8) sample. The area of EDX map acquisition is marked by a white rectangle. Ga and Al are present as oxides, the Ag nanoparticles appear in their metallic form.

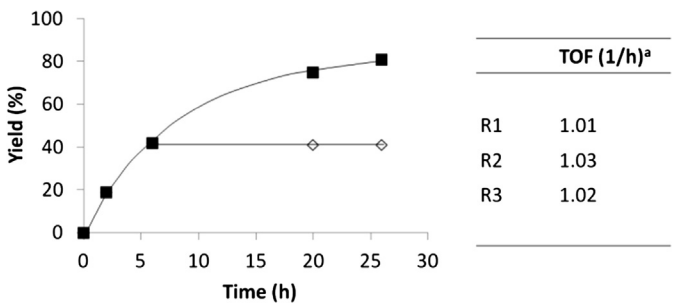


Fig. 6. Right: ^a Turnover frequency (TOF = mole of product formed per mole of Ag per h based on GC analysis of the reaction mixture after 26 h of reaction) for the $\text{Ag}/\text{Al}_2\text{O}_3-\text{Ga}_2\text{O}_3$ (0.8) catalyst in three runs: R1, R2 and R3. Left: hot filtration experiment: after 6 h, the reaction liquid without the catalyst was allowed to react further (\diamond). For comparison, the yield with the Ag catalyst is also displayed (\blacksquare). Reaction conditions: 3 mol% Ag catalyst, 0.5 mmol NaH, 1 mL toluene, **1** (3.6 mmol), **2** (1.8 mmol), 110 °C, Ar.

adsorption sites for the amine, bringing this reactant in close contact with the aldehyde formed on the Ag sites. Finally, Lewis acids have previously been shown to accelerate the imine reduction step of the hydrogen borrowing cycle [16]. Besides enhanced Lewis acidity, Ga_2O_3 could potentially also contribute by its redox properties, allowing it to adsorb hydrides, which could also facilitate the imine reduction step [27,28].

Close inspection of the results in the series of mixed oxides (Table 4) shows that an increasing Ga content leads to higher TOFs (entries 3–5). TEM showed that $\text{Ag}/\text{Al}_2\text{O}_3-\text{Ga}_2\text{O}_3$ (0.3) and $\text{Ag}/\text{Al}_2\text{O}_3-\text{Ga}_2\text{O}_3$ (0.8) display a similar mean Ag particle size of 8 ± 1 nm (see supporting information). Hence particle size does not explain the activity differences. The highest TOF was obtained for the $\text{Ag}/\text{Al}_2\text{O}_3-\text{Ga}_2\text{O}_3$ (0.8) catalyst (entry 5). At this high Ga content, potential interactions between Ag sites and Lewis acid sites are maximized, while the remaining Al ensures a high surface area. The pure, Ag-free supports were not catalytically active; they hardly showed any conversion (<1%) for the alcohol amination reaction.

The best catalyst, $\text{Ag}/\text{Al}_2\text{O}_3-\text{Ga}_2\text{O}_3$ (0.8), was tested on other substrates. As in literature often only aniline or aniline derivatives are used, sufficient attention was given to the variation of the amine (Table 5). Generally, good amine conversions were obtained with the catalyst, though with the aliphatic alcohols, the catalysts reacted more slowly (entries 8–10). Using benzylic or aliphatic amines (entries 4, 6 and 7), the secondary amine:imine ratio became lower compared to those obtained for aniline substrates (entries 1–3 and 8–9) due to the higher stability of the imine. When coupling two aliphatic reagents, only the imine was formed (entry 10). For none of the reactions, tertiary amines were detected, not even for the aliphatic substrates, probably due to the application of mild reaction conditions. Noticeable are also the small amounts of amides encountered in some reaction mixtures (entries 4, 7–10), indicating that the intermediate hemiaminal, formed through reaction between the aldehyde and the amine [16], sometimes undergoes a dehydrogenation, rather than a dehydration. In the case of morpholine as substrate, the amide was even the dominant product (entry 5), which has also been observed by others when using $\text{Ag}/\text{Al}_2\text{O}_3$ catalysts [20,29]. Besides the formation of amides, traces of the aldehyde formed by the dehydrogenation of the alcohol were also encountered as side product at high amine conversions. When comparing the performance of this catalytic system with other Ag catalysts used in literature [16,20], generally, similar yields are obtained for similar reactions, but with the advantage that mild reaction conditions can be applied.

Finally, the recyclability of the catalysts was tested. As can be seen from Fig. 6, the catalyst can be used at least three times without loss in activity. Further, to check the heterogeneity of the reaction, a hot filtration test was performed (Fig. 6). After removal

of the catalyst, the yield remained identical even after 20 h of reaction, indicating that Ag does not leach to the reaction liquor during reaction to homogeneously perform the reaction.

4. Conclusions

Ag nanoparticles, formed by the reduction of AgNO_3 in the presence of NaH show high selectivity for the desired secondary amine in a reference alcohol amination reaction using mild reaction conditions (110°C , 20 h). NaH is not only necessary to reduce the silver salt, but also plays a role in the reaction mechanism by activating the alcohol for subsequent oxidation by the Ag nanoparticles. In an attempt to enhance their stability, a series of mixed $\text{Al}_2\text{O}_3\text{-Ga}_2\text{O}_3$ supports were synthesized to immobilize the particles. The supported Ag catalysts show higher turnover frequencies when immobilized on the mixed $\text{Al}_2\text{O}_3\text{-Ga}_2\text{O}_3$ supports compared to the pure alumina supports. This is related to the higher surface density of strong Lewis acidic sites compared to pure alumina, caused by the presence of Ga. The mixed oxides with a higher Ga content display higher turnover frequencies and the best results were obtained with the support with a $\text{Ga}/(\text{Ga} + \text{Al})$ ratio of 0.8, for which TEM investigations revealed a close interaction between the Ag species and the Ga_xO_y phase. The catalyst proved active for the alcohol amination of a variety of aliphatic and aromatic amines using mild reaction conditions and remained active in at least three runs without loss in activity.

Acknowledgements

IG and ST thank the Research Foundation Flanders (FWO) for financial support as research assistant and postdoctoral researcher respectively, and under project number G004613N. We are also grateful to IWT for support in the SBO project MAPIL, to the federal government for support in IAP-PAI P7/05 project and to the KU Leuven for the Methusalem grant CASAS.

Appendix A. Supplementary data

Supplementary data associated with this article can be found, in the online version, at <http://dx.doi.org/10.1016/j.apcata.2013.09.044>.

References

- [1] Y.J. Chang, T.J. Chow, *Tetrahedron* 65 (2009) 9626–9632.
- [2] B. Schlummer, U. Scholz, *Adv. Synth. Catal.* 346 (2004) 1599–1626.
- [3] S. Lengvinaite, J.V. Grazulevicius, S. Grigalevicius, B. Zhang, J. Yang, Z. Xie, L.X. Wang, *Synth. Met.* 158 (2008) 213–218.
- [4] M.R. Dobler, I. Bruce, F. Cederbaum, N.G. Cooke, L.J. Diorazio, R.G. Hall, E. Irving, *Tetrahedron Lett.* 42 (2001) 8281–8284.
- [5] F.B. Koyuncu, S. Koyuncu, E. Ozdemir, *Electrochim. Acta* 55 (2010) 4935–4941.
- [6] A. Guram, R. Rennels, S. Buchwald, *Angew. Chem. Int. Ed.* 34 (1995) 1348–1350.
- [7] J. Louie, J. Hartwig, *Tetrahedron Lett.* 36 (1995) 3609–3612.
- [8] I. Geukens, J. Fransaer, D.E. De Vos, *ChemCatChem* 3 (2011) 1431–1434.
- [9] S. Bähn, S. Imm, L. Neubert, M. Zhang, H. Neumann, M. Beller, *ChemCatChem* 3 (2011) 1853–1864.
- [10] G. Guillena, D.J. Ramón, M. Yus, *Chem. Rev.* 110 (2009) 1611–1641.
- [11] A. Martínez-Asencio, D.J. Ramón, M. Yus, *Tetrahedron* 67 (2011) 3140–3149.
- [12] R. Martinez, D.J. Ramón, M. Yus, *Org. Biomol. Chem.* 7 (2009) 2176–2181.
- [13] K.-i. Shimizu, K. Kon, W. Onodera, H. Yamazaki, J.N. Kondo, *ACS Catal.* 3 (2013) 112–117.
- [14] J. Sun, X. Jin, F. Zhang, W. Hu, J. Liu, R. Li, *Catal. Commun.* 24 (2012) 30–33.
- [15] X. Cui, X. Dai, Y. Deng, F. Shi, *Chem. -Eur. J.* 19 (2013) 3665–3675.
- [16] K. Shimizu, M. Nishimura, A. Satsuma, *ChemCatChem* 1 (2009) 497–503.
- [17] K. Shimizu, K. Sugino, K. Sawabe, A. Satsuma, *Chem. -Eur. J.* 15 (2009) 2341–2351.
- [18] K.-i. Shimizu, K. Shimura, M. Nishimura, A. Satsuma, *RSC Adv.* 1 (2011) 1310–1317.
- [19] X. Cui, Y. Zhang, F. Shi, Y. Deng, *Chem. -Eur. J.* 17 (2011) 1021–1028.
- [20] H. Liu, G.-K. Chuah, S. Jaenicke, *J. Catal.* 292 (2012) 130–137.
- [21] T. Watanabe, Y. Miki, Y. Miyahara, T. Masuda, H. Deguchi, H. Kanai, S. Hosokawa, K. Wada, M. Inoue, *Catal. Lett.* 141 (2011) 1338–1344.
- [22] I. Geukens, E. Plessers, J.W. Seo, D.E. De Vos, *Eur. J. Inorg. Chem.* (2013) 2623–2628.
- [23] M. Haneda, E. Joubert, J.-C. Menezo, D. Duprez, J. Barbier, N. Bion, M. Daturi, J. Saussey, J.-C. Lavalle, H. Hamada, *Phys. Chem. Chem. Phys.* 3 (2001) 1366–1370.
- [24] A.L. Petre, A. Auroux, P. Gélin, M. Calderaru, N.I. Ionescu, *Thermochim. Acta* 379 (2001) 177–185.
- [25] T. Masuda, T. Watanabe, Y. Miyahara, H. Kanai, M. Inoue, *Top. Catal.* 52 (2009) 699–706.
- [26] S. Handjani, E. Marceau, J. Blanchard, J.-M. Krafft, M. Che, P. Mäki-Arvela, N. Kumar, J. Wärnå, D.Y. Murzin, *J. Catal.* 282 (2011) 228–236.
- [27] W. Jochum, S. Penner, K. Föttinger, R. Kramer, G. Rupprechter, B. Klötzer, *J. Catal.* 256 (2008) 268–277.
- [28] S.E. Collins, M.A. Baltañás, A.L. Bonivardi, *Langmuir* 21 (2004) 962–970.
- [29] K.-i. Shimizu, K. Ohshima, A. Satsuma, *Chem. -Eur. J.* 15 (2009) 9977–9980.